

Effect of thermal conditioning on the initiation threshold of secondary high-explosives

A. Maiti, W. L. Shaw, S. M. Clarke, C. Fox, L. A. Ke, W. N. Cheung, M. A. Burton, G. D. Kosiba, C. D. Grant, R. H. Gee

September 12, 2023

Propellants, Explosives, Pyrotechnics

Disclaimer

This document was prepared as an account of work sponsored by an agency of the United States government. Neither the United States government nor Lawrence Livermore National Security, LLC, nor any of their employees makes any warranty, expressed or implied, or assumes any legal liability or responsibility for the accuracy, completeness, or usefulness of any information, apparatus, product, or process disclosed, or represents that its use would not infringe privately owned rights. Reference herein to any specific commercial product, process, or service by trade name, trademark, manufacturer, or otherwise does not necessarily constitute or imply its endorsement, recommendation, or favoring by the United States government or Lawrence Livermore National Security, LLC. The views and opinions of authors expressed herein do not necessarily state or reflect those of the United States government or Lawrence Livermore National Security, LLC, and shall not be used for advertising or product endorsement purposes.

Effect of thermal conditioning on the initiation threshold of secondary high-

explosives

Amitesh Maiti,* William L. Shaw, Samantha M. Clarke, Christie Fox, Lucia A. Ke, William N. Cheung,

Mark A. Burton, Graham D. Kosiba, Christian D. Grant, Richard H. Gee

Lawrence Livermore National Laboratory, Livermore CA 94550

*corresponding author: amaiti@llnl.gov

Abstract:

While most performance metrics of high-explosive based devices like detonation velocity, detonation

pressure, and energy output are expected to degrade over time, the evolution of initiation threshold appears

less clear, with claims of both increasing and decreasing trends in threshold having been made in the

literature. This work analyzes D-optimally designed sequential binary test data for a few thermally

conditioned porous-powder and polymer-bonded HE initiator systems using a Bayesian likelihood method

employing the probit regression model. We find that in most cases the initiation threshold decreases (i.e.,

sensitivity increases) upon accelerated thermal conditioning. However, such results are nuanced and

influenced by factors like the contact area of initiating stimulus, HE characteristics like density and specific

surface area, as well as possible thermally induced changes to other materials and interfaces involved.

Keywords: Initiation Threshold, Initiation Sensitivity, Thermal conditioning, Likelihood, Probit regression

1. Introduction

High explosives are energetic materials usually in the form of molecular crystals, where each molecule comprises both oxidizer and fuel-incorporating functional groups [1, 2]. Having the oxidizer and fuel within the same molecular component is key to powerful detonations that have become indispensable in construction/demolition engineering, welding, automotive airbags, mining, military, and other applications. In a typical detonator system the detonation process begins with an initiation train that consists of one or more secondary HEs, which are powerful, but insensitive energetic materials that (for impact initiation) can only be initiated through stimulus of critical size, shape and strength of the impactor. Such design is mandated by safety and control requirements to prevent unintended detonation related accidents and hazards. While there are different types of detonator-system designs, two most common ones, especially relevant for secondary HE systems, are the Exploding Bridge Wire (EBW) and the Exploding Foil Initiators (EFI) [3, 4]. In the EBW design a metal bridge wire is in direct contact with porous secondary HE, typically pressed to around 50% of crystalline density. Initiation in such devices is believed to occur through shock waves generated when the bridge wire is made to explode. EFI designs on the other hand converts electrical energy from a high voltage capacitor discharge into intense localized heat, which instantly vaporizes a metal foil into a high-pressure plasma that pushes a polymer film (typically polyimide), commonly referred to as a 'flyer' or 'slapper'. The flyer accelerates through a gap and directly impacts a high-density HE pellet with high velocity, and the resulting shock wave leads to detonation. In either design the initial explosion of the wire or foil is carried out by the application of a voltage in a control circuit, referred to below as 'firing voltage' for simplicity. In many applications the HE pellet is typically an energetic material slurry-coated with a few weight percent of a polymer-binder and pressed to a high density (> 90% of the corresponding crystalline density). Henceforth we refer to such polymer-bonded explosive system as a PBX. When working with such high-energy devices two complementary aspects of high importance are safety and performance. While safety encompasses prevention of accidental explosive ignition, performance hinges on successful detonation at high enough firing voltages.

In many applications the systems are stored or fielded for extended periods of time. It is thus of great interest to know how the safety and performance characteristics of such devices change in the long term [5,

6]. While performance characteristics such as function time [4, 6, 7], detonation pressure, and output energy are expected to degrade over time, the evolution of the initiation sensitivity of the HE or the detonator assembly is not clear. For instance, in EBW studies on low-density powder pressings of PETN Dinegar and co-workers [8] have observed a positive correlation between initiation threshold voltage and flow-permeable specific surface area (FSSA). Given that thermal conditioning causes gradual reduction in FSSA [5, 6, 7, 9], the above implies decreasing initiation threshold voltage (i.e., increasing initiation sensitivity) over time. A recent large-scale study on PETN powder [10] also indicate similar behavior, although the thermally induced reduction in initiation threshold voltage in this study was not statistically significant. This was perhaps due to limited conditioning (1 month at 75°C) and would likely have been significant with longer duration and/or higher conditioning temperatures. In contrast, independent EFI studies with PBX PETN based initiators [11] found an increase in the initiation threshold (i.e., decrease in initiation sensitivity) with thermal conditioning. A recent study [12] found the same effect in a Hexanitrostilbene (HNS) and HMX-based EFI system, although the increase in initiation threshold was found to be non-monotonic as a function of time. In light of the above discussion, we wanted to analyze available initiation-test data on various systems obtained over the years in our group, with the hope of shedding deeper light into this important problem.

The rest of the paper is organized as follows. In section 2 we provide a brief discussion of D-optimally designed sequential binary tests in general and our method of analyzing such data to determine a point estimate of the initiation threshold and the associated statistical uncertainty (i.e., confidence margins). In section 3 we analyze experimentally measured sensitivity data for a few thermally conditioned systems, including two EBW applications (one using HMX and the other using PETN) and three EFI applications (all using PETN based PBX). For the EBW systems the whole component (including the HE and the metal bridge wire) was thermally conditioned, while for the EFI systems we considered situations where: (1) only the PBX material was conditioned, (2) only the (polyimide-based) flyer was conditioned, and (3) the entire EFI component was conditioned. Finally, in Section 4 we attempt to provide some rationalization of our findings, although the physics of detonation is admittedly complex, and our understanding is far from complete.

2. D-optimal design of sequential binary data and initiation threshold

Let us consider a set of n similar HE systems that are sequentially fired at voltages V_i (i = 1, 2, ..., n). Let the corresponding binary observations of successful (GO) and unsuccessful (NOGO) detonation be encoded in variable $\{y_i\}$ (y = 1/0 for GO/NOGO). The likelihood (L) of the observed data is given by:

$$L \propto \prod_{i=1}^{n} p_i^{y_i} (1 - p_i)^{1 - y_i}, \tag{1}$$

where p_i is the probability of successful initiation at firing voltage V_i . In a probit regression setting the initiation probabilities $\{p_i\}$ are modeled as:

$$p_i = \Phi(\beta_0 + \beta_1 V_i) \,, \tag{2}$$

where Φ is the cumulative distribution function (cdf) of the standard normal distribution, and (β_0, β_1) are probit regression coefficients. Neyer [13] expressed eq. (2) in the form,

$$p_i = \Phi((V_i - \mu)/\sigma), \qquad (3)$$

where μ is the 50% threshold voltage, i.e., the firing voltage at which the probability of initiation is 50%, and σ is a 'scale parameter' that controls how fast the initiation probability changes with change in the firing voltage around μ . In the following we loosely refer to μ as the 'initiation threshold voltage' or 'initiation threshold' or simply 'threshold'. Comparing eq. (2) and (3) we obtain the relations: $\mu = -\beta_0/\beta_1$ and $\sigma = 1/\beta_1$. When transforming from the variables (β_0, β_1) to variables (μ, σ) the Jacobian of transformation is $1/\sigma^3$, i.e., $\iint d\beta_0 d\beta_1 \to \iint \sigma^{-3} d\mu d\sigma$.

For reliable determination of initiation threshold, it is important to design the firing voltages such that μ can be determined with minimum uncertainty for a given number of shots. To address this problem, Neyer proposed a D-optimal design, i.e., one in which each V_i is chosen such that it maximizes the Fisher information [14] of the first i shots. Such design was shown to be an improvement over previous methods, e.g., the Bruceton, Robbins-Monroe, and the Langley methods [15-17]. To use the D-optimal scheme, it is first necessary to establish overlap, i.e., observe a NOGO response at a voltage higher than a GO response.

Although Neyer's SenTest software [18] provides an algorithm for establishing overlap, in our experiments we found it more efficient to use domain knowledge to obtain overlap within a reasonably few (~ 8 or even fewer) shots. Once overlap is achieved, the remaining voltages are chosen according to the D-optimal scheme [13, 18].

Once a desired number of shots have been fired (15-30 shots in all data discussed in this paper), it is common procedure to determine (β_0 , β_1) or equivalently (μ , σ) by the maximum likelihood estimate (MLE), i.e., determine parameter values that maximize likelihood L. One then performs uncertainty quantification using the inverse of the Fisher Information matrix. This procedure is accurate when the number of shots is large. Given that we are often resource-limited, and often work with a D-optimal series of as few as 15 shots, we adopt a more general Bayesian approach in which we use the Likelihood (eq. (1) and (2)) to construct a posterior probability density function (pdf) of μ . More specifically, with no prior information, we construct the following posterior joint pdf of (μ , σ):

$$f_{ioint}(\mu, \sigma) \propto \prod_{i=1}^{n} \Phi((V_i - \mu)/\sigma)^{y_i} \{1 - \Phi((V_i - \mu)/\sigma)\}^{1-y_i}$$
. (4)

We then integrate out σ to obtain the following marginal distribution of μ :

$$f_{marginal}(\mu) = C \int_0^\infty f_{joint}(\mu, \sigma) \, \sigma^{-3} d\sigma \,, \tag{5}$$

where C is a normalization constant and the σ^{-3} factor corresponds to the Jacobian of transformation as discussed earlier. Once the marginal distribution is obtained, we can determine any statistic for μ , including mean, mode, and confidence interval (CI). Below we will specifically make frequent use of two summary quantities for μ , i.e., (1) maximum (or mode) of $f_{marginal}$, commonly referred to in the Bayesian literature as the maximum-a-posteriori (MAP) [19] estimate, and (2) the 90% CI as determined from the 5th and 95th percentiles of $f_{marginal}$.

Before proceeding to the analysis of experimental data, a justification of the (Bayesian) Likelihood methodology used here is in order. For instance, instead of $f_{marginal}$, which requires integration over σ , why not determine CI by the standard formula $\mu_{MLE} \pm z_{\alpha/2} \sigma_{MLE}/\sqrt{n}$ for CI (where n is the number of shots, α

the level of significance, and $z_{\alpha/2}$ the 100(1 – $\alpha/2$)% quantile of the standard normal distribution)? To this point we would like to add that: (1) although the probit regression model (as employed here) is equivalent to assuming that the sample-to-sample variation in initiation threshold follows a Normal distribution with parameters (μ, σ^2) , one can never directly measure the initiation threshold value of any specific physical sample. Thus, when employing binary GO/NOGO experiments one expects greater uncertainty in the parameters (μ, σ^2) than for properties that could be directly measured; and (2) for the case of small number of shots (~ 15-30 as employed in all studies reported here) we often see a wide distribution of (μ, σ^2) about the MLE point that is often not normal-like or even symmetric. Thus, determining symmetric confidence limits based on just the MLE point may not be appropriate. In all cases we find that the CI constructed by the Likelihood method is wider than that predicted by the standard formula, i.e., our method naturally incorporates the higher uncertainty due to direct unobservability of initiation threshold. Furthermore, through a prior term it can organically include any previous/domain knowledge about the system sensitivity, which can to some degree assuage uncertainties due a limited number of shots. In cases where a strong correlation between initiation sensitivity and observed microstructure can be established, it is possible to include that in the model through additional terms involving microstructure summary variables [11, 20-25]. However, such data require significant experimental efforts, and in most cases are not available.

In the next section we make use of $f_{marginal}$ (eq. (5)) to study the effect of thermal conditioning on μ . More specifically, we use overlaps (or lack thereof) of the $f_{marginal}$ distributions of pre- and post-conditioned systems to judge statistical significance of thermally induced change. We would like to point out that the experimental design method discussed here is appropriate for determining $\sim 50\%$ threshold of initition, i.e., close to the middle of the response curve. Determining extreme quantile thresholds (e.g., 0.01% thresholds as in 'safety' problems, or 99.9% thresholds as in 'performance' scenarios) are more challenging, and are being addressed in the literature [26, 27].

3. Thermal conditioning effect on initiation threshold voltage

We now make use of the analysis method outlined in the previous section for various datasets. More specifically, to follow up on varied observations regarding thermally induced effects on initiation threshold in the literature (as discussed in section 1), we chose to analyze D-optimally designed sequential test data for EBW or EFI systems employing three different HE systems: (i) porous PETN powder pressed to $\sim 50\%$ porosity (EBW); (ii) porous HMX powder pressed to $\sim 50\%$ porosity (EBW); and (iii) high-density PETN based PBX (EFI).

Table 1 lists five different conditioning studies analyzed here with some details regarding the type of detonator and HE deployed, thermal conditions, number of test fire shots implemented, etc. We note that thermal conditioning in all these studies were carried out at elevated temperatures (and in some cases elevated humidity levels) with the hope of estimating long-term (e.g., decades under ambient storage conditions) effects using shorter-term experiments. The first two studies employed EBW detonators using porous-powder HMX and PETN, respectively, while studies 3 and 4 were performed on EFI detonators (flyer sizes ~ 0.6 mm square) both employing high-density PETN based PBX. Study 5 was aimed at exploring the effects of smaller flyer sizes (0.2 mm square) on initiation sensitivity. We would like to note that these were all disparate studies using different firing electrical circuits and different thermal conditions and were not systematically designed with the current analysis in mind. The idea behind the present work was to analyze such diverse data to glean some broad conclusions on thermally induced effects on initiation threshold with the aim of validating or clarifying observed conditioning effects in the literature. Given that the initiation threshold voltage is not just material-depedent but depends strongly on the firing circuit as well, and different firing circuits were employed in different studies, we chose to 'normalize' the results for each study by expressing them in terms of ratio (percent) to the MAP estimate of the initiation threshold of the corresponding unconditioned system.

Figure 1 relates to study 1 indicated in Table 1, i.e., an HMX powder pressed to ~50% porosity in which the whole EBW component was subjected to conditioning at elevated temperatures of 75°C and 95°C and two different humidity levels, i.e., 'dry' (< 10% relative humidity) and 'wet' (~ 45% RH). The 95°C study

was carried out for 8 weeks, while the 75°C study was carried out for 32 weeks. Fig. 1(a) plots the $f_{marginal}$ distributions of initiation threshold μ for various thermal conditions, while Fig. 1(b) displays the corresponding MAP estimates (small circles) and the 90% confidence interval (vertical error bars). From the results of Fig. 1 we see that: (1) the initiation threshold decreases (i.e., sensitivity increases) with accelerated thermal conditioning in a statistically significant way; (2) humid conditions enhance the thermally induced change in initiation threshold, as do higher conditioning temperature, which is to be expected. For the conditioning study at 75°C under dry conditions we have also performed sensitivity tests at a few intermediate times, i.e., 2, 4, 8, 16 weeks to monitor how the initiation threshold evolves as a function of conditioning time at these elevated temperatures. These results are summarized in Fig. 2, where points (i.e., small circles) indicate the MAP estimate of initiation threshold and error bars indicate the 90% CI computed from $f_{marginal}$ distributions. We see that there is an overall decreasing trend in the initiation threshold as a function of time, although due to wide confidence intervals (i.e., large error bars) the change is statistically not significant until after 16 weeks of conditioning. We would like to note that although the MAP estimate of the initiation threshold is robust, the uncertainty (in terms of confidence interval width) appears to be a sensitive function of the chosen firing voltages as well as the observed outcomes, especially for the small number of samples employed here in each test series. Thus, we observe large fluctuations in the confidence interval width, with the uncertainty in the 8-week data being especially large.

Figure 3 displays results of study 2, i.e., a porous-powder PETN system for which the whole EBW was conditioned for 2 years at 40°C. It appears that there is no statistically significant changes to threshold until after 24 months when a decreasing trend is detected. Given that with thermal conditioning the FSSA of porous powders are known to decrease, the results of studies 1 and 2 are consistent with previous observations [9] of threshold changes as a function of FSSA.

Results of study 3 are displayed in Fig. 4. This was a study in which PETN based PBX was used as the initiating HE within an EFI device, and only the HE pressings were conditioned. Conditioning was performed at low humidity under two different temperatures, i.e., for 120 days at 40°C and for 87 days at 75°C. Fig. 4 indicates a thermally induced lowering of the initiation threshold voltage, the change being statistically more significant under more severe conditions.

Figure 5 displays results of study 4, in which only the flyer material in an EFI system using PETN based PBX was conditioned (~ 57 hours at 72°C under 50% RH). The conditioning of the flyer in this case leads to a statistically significant lowering of the initiation threshold. Thus, each of the first four studies indicate the same overall trend, i.e., an thermally induced lowering of the initiation threshold (i.e., increase in initiation sensitivity), which gets exacerbated in the presence of moisture. However, as mentioned in the Introduction section, the opposite behavior has also been observed in some systems. More specifically, a recent sensitivity study on PETN based EFI detonators found statistically significant increase in initiation threshold due to thermal conditioning [11]. An important aspect of this work was that it employed much smaller flyer dimensions (~ 0.2 mm).

In study 5 we analyze sensitivity test data on EFI systems with 0.2 mm flyers using PETN based PBX, with results displayed in Fig. 6. In this study the whole detonator component (i.e., HE + flyer) was conditioned for two months at 80°C under dry (< 10% RH) and humid (~ 30% RH) conditions, referred to as 'T_Cond' and 'T&H_Cond', respectively. From Fig. 6 it appears that thermal conditioning significantly increases threshold, i.e., lowers initiation sensitivity, while humidity appears to exacerbate the effect by a small amount. The significantly different results in EFI study 5 as compared to EFI studies 3 and 4 is evidence of the importance of flyer size. The importance of spot-size has been mentioned in previous works as well [28].

Before we attempt to summarize and understand the above results on initiation threshold, one comment on accelerated conditioning is in order. The idea behind using elevated temperatures is that conditioning for time t at an elevated temperature T is deemed to be equivalent to conditioning for a much longer time (i.e., $a_T t$, where $a_T \gg 1$ is the corresponding acceleration factor) under long-term ambient storage conditions. Assuming an Arrhenius model, the acceleration factor is governed by an activation energy barrier, which is dependent on the system under consideration. For systems with a single dominant evolution mechanism (i.e., involving a single activation barrier) the acceleration factor is easy to determine. This assumption is behind methods such as time-temperature superposition (TTS) that involves rigid-shifting of elevated-temperature isotherms along logarithmic timescales to create long-term prediction curves under ambient storage conditions [29-32]. However, for any real multicomponent systems, as is the case with either EBW or EFI

detonators, one needs to be cognizant of the fact that many different mechanisms are at play, and there may not be a single dominant activation barrier. It is to be noted that the conditioning in the above studies were performed at different temperatures for varied durations. However, we did not attempt to convert the accelerated evolution into 'equivalent' times under ambient storage conditions. Our intent in this work was simply to identify statistically significant changes in the initiation threshold and the direction of such change under accelerated conditions.

4. Summary and Discussion

Through likelihood analysis on probit regression model of sequential binary data we found several interesting effects of thermal conditioning on the initiation threshold voltage, including: (1) for porous powder based EBW systems, the initiation threshold decreases (i.e., sensitivity increases) with conditioning of the whole device. Given past knowledge that initiation threshold of just the HE part decreases with thermal conditioning [8], the above implies that conditioning of other material components (e.g., metal bridge wire and other accessorial parts) either also decreases or does not significantly affect initiation threshold; (2) for PBX based EFI systems with larger-sized (0.6 mm) flyers conditioning also appears to lower initiation threshold voltage irrespective of whether the HE component or the flyer is conditioned; however such effect can be quantitatively altered or even reversed when small (0.2 mm) flyers are used; (3) humidity appears to exacerbate changes due to thermal conditioning. These results help put in perspective previous claims in the literature where both increase and decrease in initiation threshold has been reported.

It is desirable to understand the above observations in terms of thermally induced microstructural and mechanical property changes to both the HE and non-HE components of the initiator system. However, this is challenging given that initiation and propagation of detonation involves complex physical and chemical processes that are not yet fully understood, despite the development of important theoretical concepts over several decades [33-38], and despite more recent grain-scale [39-45], multi-scale [46], atomistic [47-51], and AI-based [52] modeling and simulations. Simplistically, one can conjecture that thermally induced coarsening leads to the formation of micro-voids (or other structural defects and inhomogeneities) of

appropriate dimensions that act as hotspots for easier initiation, i.e., lower threshold. For PBX systems subtle changes to the grain-scale microstructure have been observed through evolution of X-ray CT summary statistics [11], although direct observation of void formation requires CT images of higher resolution. Added to the complexity is the fact that the chemical composition of the polymeric binder (in PBX systems) can have a significant effect on sensitivity as measured by the gap test while shock response of polymer binders in general is far from understood [53].

Study 4 (in section 3) was designed to isolate the effect of thermally induced effects within the polyimide flyer. However, initiation depends not only on the mechanical strength of the flyer but also on its shape and speed at the time of impact. To obtain further insights into this we have recently imaged various EFIs in action using a fast-framing camera and measured the flyer velocity using photon Doppler velocimetry (PDV). These images show that the velocity and shape characteristics of the flyers are relatively unchanged under the thermal/humidity conditions presented here. Thus, the observed decrease in initiation threshold in Fig. 5 could perhaps be attributed to a thermally induced enhancement in the mechanical strength of the flyer, possibly due to cross-linking or other chemically induced changes in the polymer film at elevated temperatures.

It is more difficult to understand and rationalize the results of study 5 that involved small flyers. In addition to spot size effects [28], it is also known that shock initiation sensitivity can vary as a function of physical characteristics of the HE itself [54], including grain-size, material density, spatial distribution and size distribution of voids, as well as the nature of the shock pulse [55]. Thus, in EFI systems with small flyers it can be surmised that even small thermally induced changes in flyer strength and shape and small microstructural changes within the PBX could affect the initiation threshold in complex ways.

Even without a full mechanistic understanding of the initiation process, it could be worth exploring phenomenological theories based on energy-fluence [56, 57] and shock-volume [58, 59] concepts to gain further insights. With the availability of appropriate microstructural data, pre- and post- conditioning, it could also become possible to construct generalized (e.g., probit or logistic) regression models that includes terms dependent on relevant summary features [11, 20-25], e.g., flow-permeable specific surface area for porous-

powder HE system, or grain-count, internal-boundary-surface-area, or surface roughness features of PBX systems.

Acknowledgement: This work was performed under the auspices of the U.S. Department of Energy by Lawrence Livermore National Laboratory under Contract DE-AC52-07NA27344.

References:

- J. P. Agrawal, High Energy Materials: Propellants, Explosives and Pyrotechnics, Wiley-VCH, Weinheim 2010.
- 2. R. Meyer, J. Köhler, A. Homburg (eds.), *Explosives*, Wiley-VCH, **2007**.
- 3. R. Varosh, Electric detonators: EBW and EFI, Propellants Explos. Pyrotech. 1996, 21, 150.
- 4. P.W. Cooper, Explosives Engineering, Wiley-VCH, New York, 1996.
- A. Maiti, R. H. Gee, Modeling growth, surface kinetics, and morphology evolution in PETN, *Propellants Explos. Pyrotech.* 2011, 36, 125.
- A. Maiti, T. Y. Olson, T. Y. Han, R. H. Gee, Long-term coarsening and function-time evolution of an initiator powder, *Propellants Explos. Pyrotech.* 2017, 42, 1352.
- M. F. Foltz, Aging of Pentaerythritol Tetranitrate (PETN), Technical Report LLNL-TR-415057, Lawrence Livermore National Laboratory, 2009.
- 8. R. H. Dinegar, The Effect of Precipitation Variables on the Specific Surface Area and Explosive Characteristics of Pentaerythritol tetranitrate, *Proceedings of the 10th International Pyrotechnics Seminar*, Karlsruhe, West Germany, **1985**, p. 13.
- 9. R. H. Dinegar, The Effects of Heat on Pentaerythritol Tetranitrate (PETN). *Proceedings of the 12th International Pyrotechnics Seminar*, Juan-Les-Pins, France, **1987**, p. 105.
- N. Lease, N. J. Burnside, G. W. Brown, J. P. Lichthardt, M. C. Campbell, R. T. Buckley, J. F. Kramer,
 K. M. Parrack, S. P. Anthony, H. Tian, S. K. Sjue, D. N. Preston, V. W. Manner, The Role of
 Pentaerythritol Tetranitrate (PETN) Aging in Determining Detonator Firing Characteristics, *Propellants Explos. Pyrotech.* 2021, 46, 26-38.
- A. Maiti, A. Venkat, G. D. Kosiba, W. L. Shaw, J. D. Sain, R. K. Lindsey, C. D. Grant, P.-T. Bremer,
 A. G. Gyulassi, V. Pascucci, R. H. Gee, Topological analysis of X-ray CT data for the recognition and trending of subtle changes in microstructure under material aging, *Comp. Matter Sci.* 2020, 182, 109782.

- 12. D.-S Kim, S.-G Jang, Study on Aging Characteristics of Exploding Foil Initiator, *J. Korean Soc. Aeronaut. Space Sci.* **2020**, *48*, 581.
- 13. B. T. Neyer, A D-optimality-based sensitivity test, *Technometrics* **1994**, *36*, 61.
- M. G. Kendall, A. Stuart, *The Advanced Theory of Statistics*, Vol. 2, Second Edition, New York: Hafner Publishing Company, 1967.
- 15. J. W. Dixon, A. M. Mood, A Method for Obtaining and Analyzing Sensitivity Data, *Journal of the American Statistical Association* **1948**, *43*, 109-126.
- H. Robbins, S. Monro, A Stochastic Approximation Method, Annals of Mathematical Statistics 1951, 29, 400.
- 17. H. J. Langlie, A Reliability Test Method For "One-Shot" Items, Technical Report ADP014612, Aeronutronic Division, Ford Motor Company, https://apps.dtic.mil/sti/citations/ADP014612, 1963.
- 18. SenTest software: http://neversoftware.com/SensitivityTestFlyer.htm.
- 19. K. P. Murphy, *Machine Learning: a Probabilistic Perspective*, MIT Press, Cambridge, Massachusetts, **2012**.
- P. Chaudhuri, P. A. Mykland, Nonlinear Experiments: Optimal Design and Inference Based on Likelihood, *Journal of the American Statistical Association*, 1993, 88, 538.
- L. M. Haines, I. Perevozskaya, W. F. Rosenberger, Bayesian-Optimal Designs for Phase I Clinical Trials, *Biometrics* 2003, 59, 591.
- A. Ivanova, K. Wang, A Non-Parametric Approach to the Design and Analysis of Two-Dimensional Dose-Finding Trials, *Statistics in Medicine* 2004, 23, 1861.
- S. Biedermann, H. Dette, W. Zhu, Optimal Designs for Dose-Response Models With Restricted Design Spaces, *Journal of the American Statistical Association* 2006, 101, 747.
- J. Karvanen, J. J. Vartiainen, A. Timofeev, J. Pekola, Experimental Designs for Binary Data in Switching Measurements on Superconducting Josephson Junctions, *Applied Statistics* 2007, 56, 167.

- 25. H. A. Dror, D. M. Steinberg, Sequential experimental designs for generalized linear models, *Journal of the American Statistical Association* **2008**, *103*, 288.
- C. F. J. Wu, Y. Tian, Three-phase optimal design of sensitivity experiments, J. Statistical Planning and Inference 2014, 149, 1.
- J. Rougier, A. Duncan, Bayesian modeling and inference for one-shot experiments, *Technometrics* 2023,
 DOI: 10.1080/00401706.2023.2224524.
- 28. J. A. Waschl, An investigation of PETN sensitivity to small scale flyer plate impact, *J. Energetic Mater*. **1998**, *16*, 279.
- 29. J.D. Ferry, Viscoelastic Properties of Polymers, 3rd ed., Wiley, New York, 1980.
- A. Maiti, A geometry-based approach to determining time-temperature superposition shifts, *Rheol. Acta* 2019, 58, 261.
- 31. A. Maiti, Second-order statistical bootstrap for the uncertainty quantification of time-temperature-superposition analysis, *Rheol. Acta* **2016**, *55*, 83.
- 32. A. Maiti, Time-temperature-superposition analysis of diverse datasets by the minimum-arclength method: long-term prediction with uncertainty margins, Rheol. Acta **2021**, *60*, 155.
- 33. F. P. Bowden, A. D. Yoffe, *Initiation and Growth of Explosion in Liquids and Solids*, Cambridge Univ. Press, **1952**.
- 34. F. P. Bowden, A. D. Yoffe, Fast Reactions in Solids, Butterworth Scientific, 1958.
- 35. R. E. Setchell, Grain-size effects on the shock sensitivity of hexanitrostilbene (HNS) explosive, *Combustion and flame* **1984**, *56*, 343.
- 36. N. K. Bourne, J. E. Field, Bubble collapse and the initiation of explosion, *Proceedings: Mathematical and Physical Sciences* **1991**, *435*, 423.
- 37. J. E. Field, Hot spot ignition mechanisms for explosives, Acc. Chem. Res. 1992, 25, 489.

- 38. C. M. Tarver, S. K. Chidester, A. L. Nichols, Critical conditions for impact-and shock-induced hot spots in solid explosives, *J. Phys. Chem.* **1996**, *100*, 5794.
- 39. C. A. Handley, B. D. Lambourn, N. J. Whitworth, H. R. James, W. J. Belfield, Understanding the shock and detonation response of high explosives at the continuum and meso scales, *Appl. Phys. Rev.* 2018, 5, 011303.
- 40. N. K. Rai, H. S. Udaykumar, Three-dimensional simulations of void collapse in energetic materials, *Phys. Rev. Fluids* **2018**, *3*, 033201.
- 41. H. K. Springer, C. M. Tarver, J. E. Reaugh, C. M. May, Investigating short-pulse shock initiation in HMX-based explosives with reactive meso-scale simulations, *Journal of Physics: Conference Series* **2014**, *500*, 052041.
- 42. R. A. Austin, H. K. Springer, L. E. Fried, Grain-scale simulation of shock initiation in composite high explosives, in *Energetic Materials From Cradle to Grave*, Springer, p 243, **2017**.
- 43. H. K. Springer, S. Bastea, A. L. Nicols, C. M. Tarver, J. E. Reaugh, Modeling the effects of shock pressure and pore morphology on hot spot mechanisms in HMX, *Propellants Explos. Pyrotech.* 2018, 43, 805.
- 44. C. D. Yarrington, R. R. Wixom, D. L. Damm, Shock interactions with heterogeneous energetic materials, *J. Appl. Phys.* **2018**, *123*, 105901.
- 45. S. Kim, Y. Wei, Y. Horie, M. Zhou, Prediction of shock initiation thresholds and ignition probability of polymer-bonded explosives using mesoscale simulations, *Journal of the Mechanics and Physics of Solids* **2018**, *114*, 97.
- 46. Y. T. Nguyen, P. K. Seshadri, O. Sen, D. B. Hardin, C. D. Molek, H. S. Udaykumar, Multi-scale modeling of shock initiation of a pressed energetic material. II. Effect of void–void interactions on energy localization, *J. Appl. Phys.* 2022, 131, 215903.
- 47. B. W. Hamilton, M. P. Kroonblawd, C. Li, A. Strachan, A hotspot's better half: non-equilibrium intramolecular strain in shock physics, *J. Phys. Chem. Lett.* **2021**, *12*, 2756-2762.

- 48. M. P. Kroonblawd, B. W. Hamilton, A. Strachan, Fourier-like thermal relaxation of nanoscale explosive hot spots, *J. Phys. Chem.* C **2021**, *125*, 20570-20582.
- 49. B. W. Hamilton, M. P. Kroonblawd, A. Strachan, The potential energy hotspot: effects of impact velocity, defect geometry, and crystallographic orientation, *J. Phys. Chem.* C **2022**, *126*, 3743-3755.
- B. W. Hamilton, M. P. Kroonblawd, A. Strachan, Extemporaneous mechanochemistry: shock-wave-induced ultrafast chemical reactions due to intramolecular strain energy, *J. Phys. Chem. Lett.* 2022, 13, 6657-6663.
- P. Das, P. Zhao, D. Perera, T. Sewell, H. S. Udaykumar, Molecular dynamics-guided material model for the simulation of shock-induced pore collapse in β-octahydro-1,3,5,7-tetranitro-1,3,5,7-tetrazocine (β-HMX), *J. Appl. Phys.* 2021, 130, 085901.
- 52. P. C. H. Nguyen, Y-T. Nguyen, P. K. Seshadri, J. B Choi, H. S. Udaykumar, S. Baek, A Physics-Aware Deep Learning Model for Energy Localization in Multiscale Shock-To-Detonation Simulations of Heterogeneous Energetic Materials, *Propellants Explos. Pyrotech.* 2023, 48, e202200268.
- 53. D. M. Dattelbaum, L. L. Stevens, Equations of State of binders and related polymers, in Static Compression of Energetic Materials, (eds) S. M. Peiris and G. J. Piermarini, Springer-Verlag, 2008.
- A. Chakravarty, M. J. Gifford, M. W. Greenaway, W. G. Proud, J. E. Field, Factors affecting shock sensitivity of energetic materials, AIP Conference Proceedings 2002, 620, 1007.
- 55. S. Watson, M. J. Gifford, J. E. Field, The initiation of fine grain Pentaerythritol Tetranitrate by Laser-Driven Flyer Plates, *J. Appl. Phys.* **2000**, *88*, 65-69.
- F. Walker, R. Wasley, A general model for the shock initiation of explosives, *Propellants Explos. Pyrotech.* 1976, 1, 73.
- 57. H. R. James, An extension to the critical energy criterion used to predict shock initiation thresholds, *Propellants Explos. Pyrotech.* **1996**, *21*, 8.

- 58. M. D. Bowden, A volumetric approach to shock initiation of Hexanitrostilbene and Pentaerythritol Tetranitrate, *AIP Conf. Proc.* **2018**, *1979*, 150004.
- M. D. Bowden, M. Maisey, A volumetric approach to shock initiation of PBX9404, AIP Conf. Proc.
 2020, 2272, 030005.

Table 1. List of various binary GO/NOGO datasets analyzed in this work.

Study #	Initiation System	Conditioned component	Thermal/Humidity Conditions	# Shots
1	Porous HMX (EBW)	Whole detonator	75°C, 95°C (Dry, Wet)	15-20
2	Porous PETN (EBW)	Whole detonator	40°C	15-20
3	PBX PETN (EFI)*	HE only	40°C, 75°C	18-20
4	PBX PETN (EFI)*	Flyer only	72°C	15
5	PBX PETN (EFI)**	Whole detonator	80°C	30

^{*}Standard flyer size (~ 0.6 mm square)

^{**}Smaller flyer size (~ 0.2 mm square)

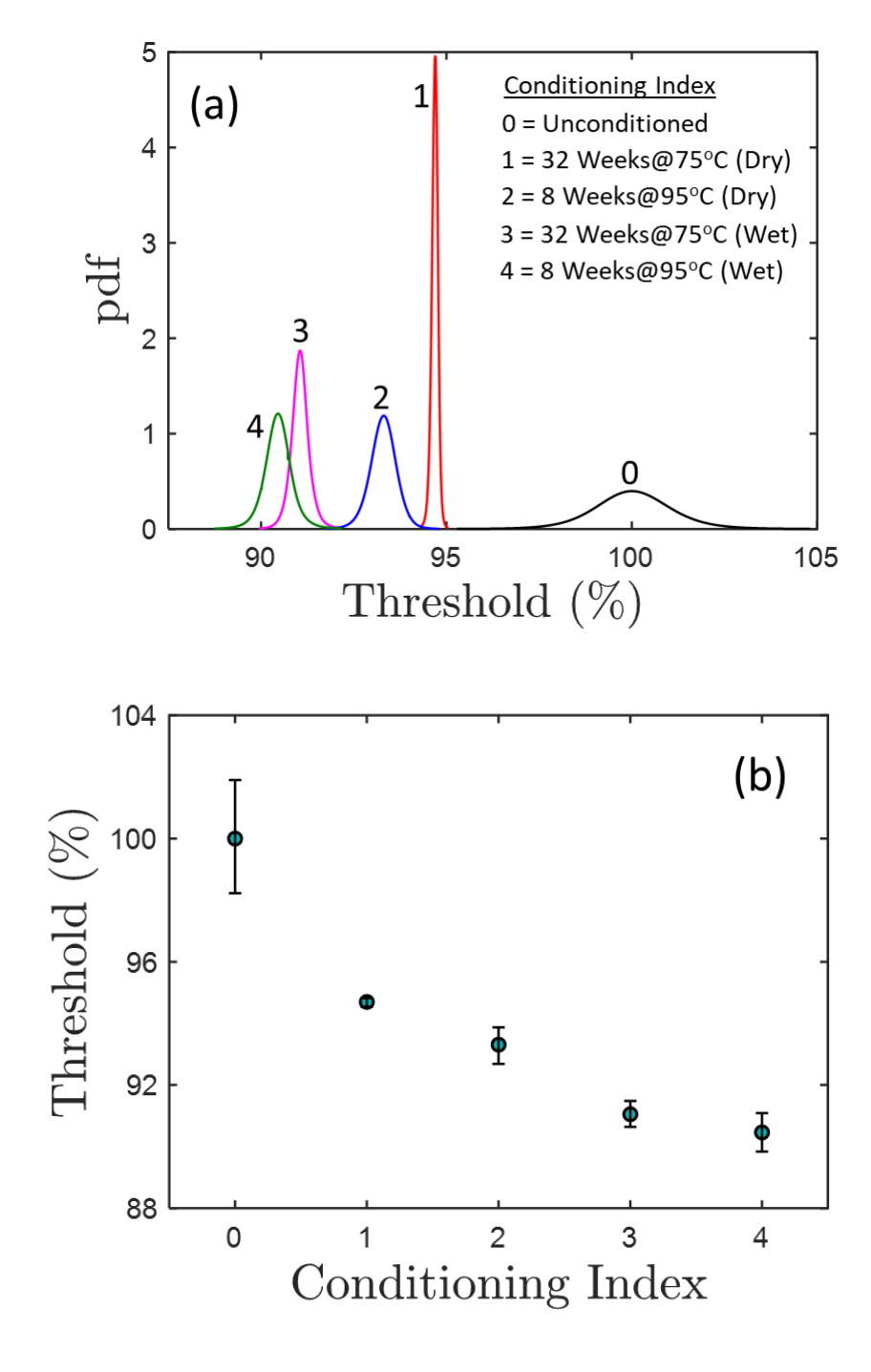


Fig. 1. Study 1: Analysis of binary test data on an EBW system based on low-density porous-HMX-powder based initiator: (a) marginal posterior pdf (uninformed prior) of initiation threshold voltage ('Threshold') for pristine and thermally conditioned powder systems, with thermal/humidity conditions indicated in plot. 'Dry' and 'Wet' represent RH levels of <10% and ~ 45%, respectively; (b) initiation threshold vs. thermal/humidity conditions, with small circles indicating the posterior maximum (MAP) and vertical bars indicating 90% confidence interval computed from posterior pdf. Accelerated thermal conditioning clearly lowers threshold, i.e., enhances initiation sensitivity, and humidity appears to exacerbate the effect. All Threshold values in this figure (and subsequent figures) are expressed as ratio to the MAP estimate of the corresponding unconditioned ('pristine') system.

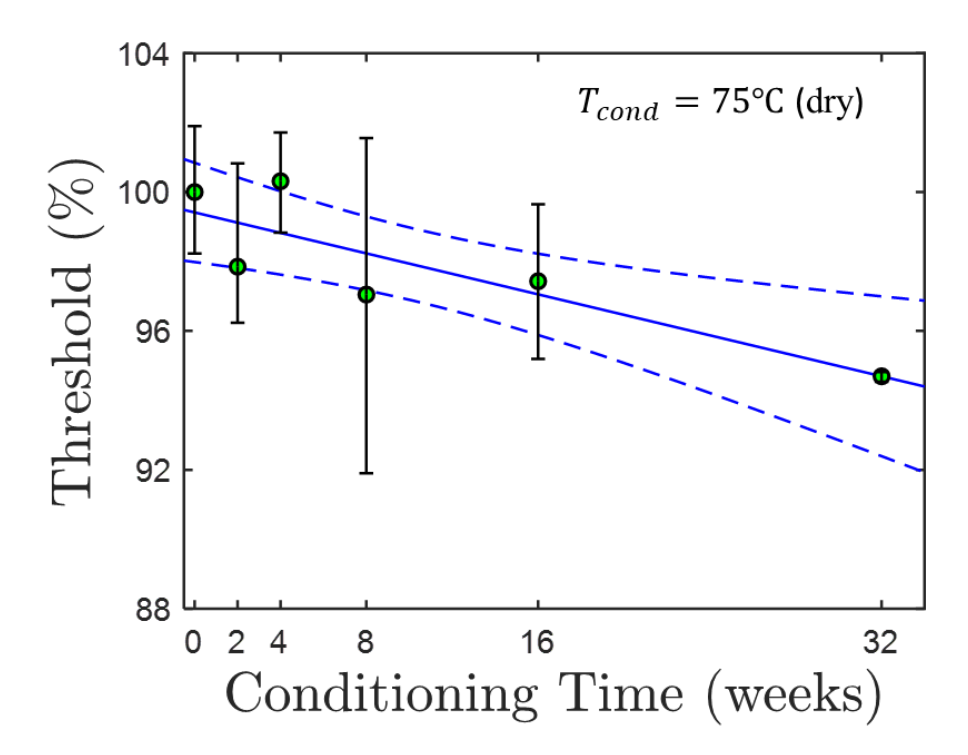


Fig. 2. Study 1: Plot of initiation threshold voltage of a HMX-powder based EBW system conditioned at 75°C (dry) for various durations (in weeks). Small circles indicate the posterior maximum (MAP) estimate, while vertical bars indicate 90% confidence interval obtained from the corresponding marginal distributions. A decreasing trend in MAP threshold as a function of conditioning time is indicated by the linear regression line (solid) with 90% prediction interval indicated by the dashed lines.

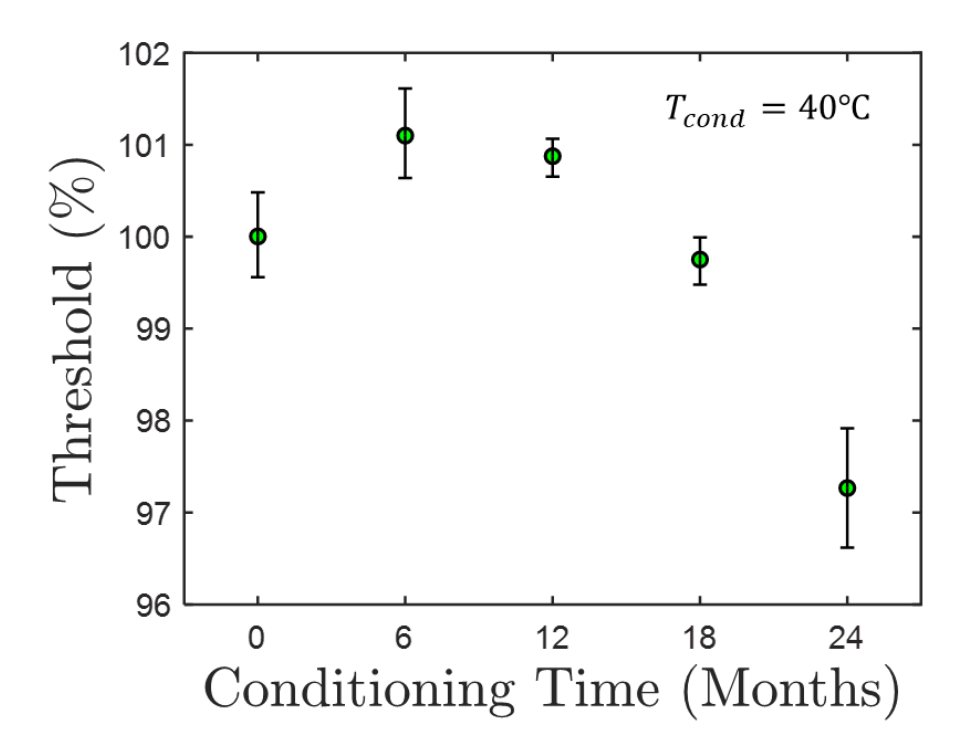


Fig. 3. Study 2: Evolution of the initiation threshold voltage of a low-density PETN-powder based EBW system that was conditioned for 2 years at 40°C: MAP estimate of threshold (small circles) along with 90% confidence margins (vertical bars) are indicated at 6-month intervals.

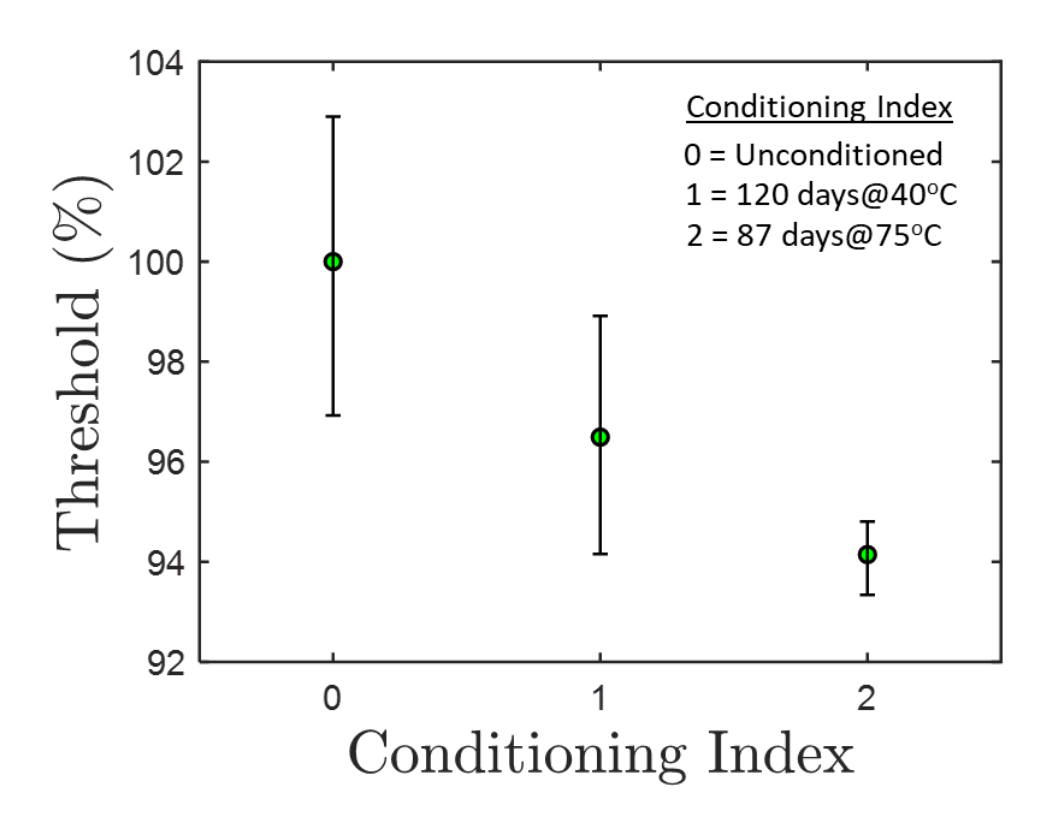


Fig. 4. Study 3: Thermal conditioning effects on the initiation threshold of an EFI system using PETN based PBX, where only the PBX material was conditioned: plots of MAP estimate of threshold (small circles) along with 90% confidence interval (vertical bars) for the unconditioned material and material under two thermal conditions. Conditioning appears to lower initiation threshold, with the rate of lowering clearly accelerated at elevated temperatures.

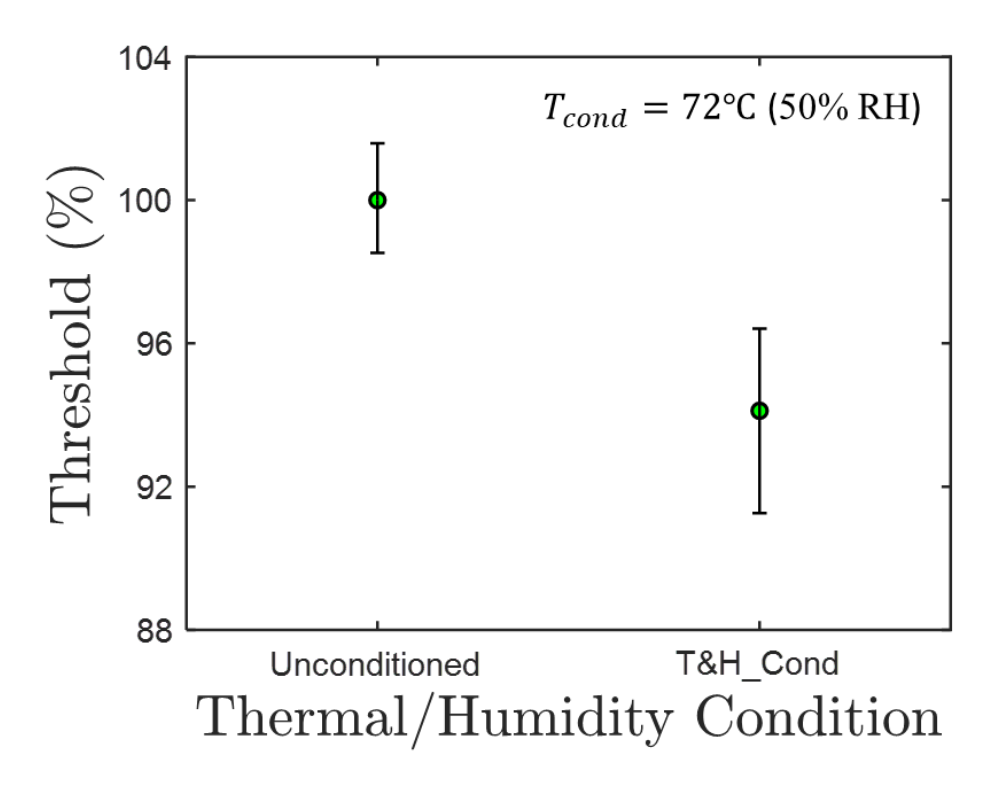


Fig. 5. Study 4: Thermal conditioning effects on the initiation threshold of an EFI system using PETN based PBX, where only the first-stage flyer was conditioned: plots of MAP estimate of threshold (small circles) along with 90% confidence interval (vertical bars) for the unconditioned system and system with flyer conditioned at 72°C under 50% RH for 57 days ('T&H_Cond'). Conditioning appears to lower threshold voltage, i.e., increase sensitivity.

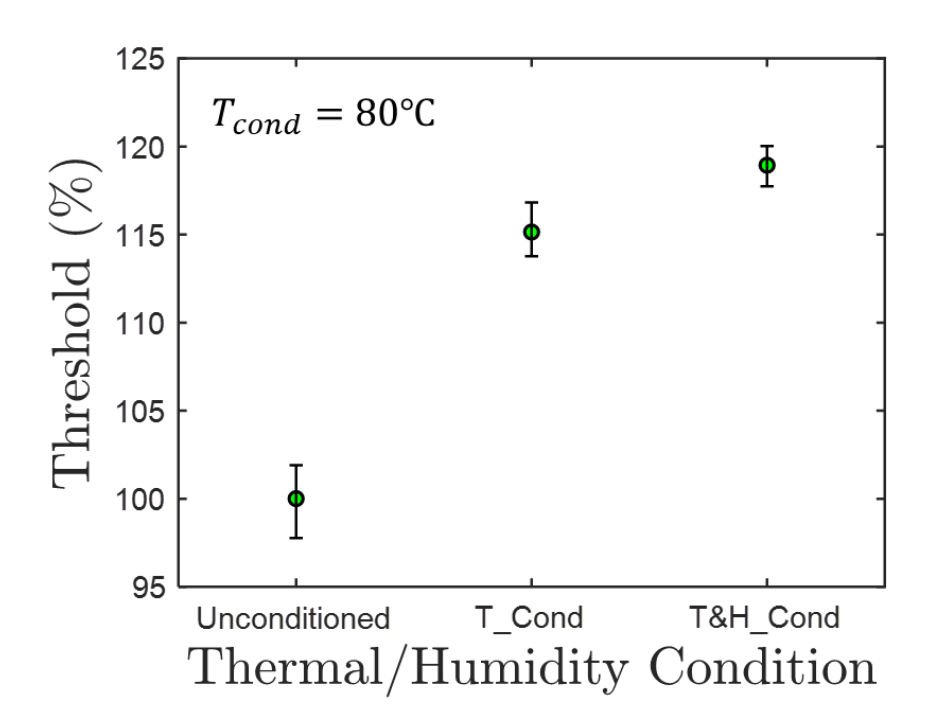


Fig. 6. Study 5: Thermal conditioning effects on the initiation threshold of an EFI system with small flyer dimensions and using PETN based PBX, where the entire component was conditioned at 80°C for 2 months under two different humidity conditions, i.e., dry ('T_Cond') and ~ 30% RH ('T&H_Cond'). Small circles indicate MAP estimate of threshold, while vertical bars indicate 90% confidence interval. Thermal conditioning appears to significantly increase threshold, i.e., lower initiation sensitivity, while humidity appears to exacerbate the effect by a small amount.